© 2022. Published by The Company of Biologists Ltd | Journal of Cell Science (2022) 135, jcs259814. doi:10.1242/jcs.259814

SHORT REPORT

A cytoplasmic protein kinase couples engagement of *Chlamydomonas* ciliary receptors to cAMP-dependent cellular responses

Mayanka Awasthi[1], Peeyush Ranjan[1], Simon Kelterborn[2,3], Peter Hegemann[2] and William J. Snell[1,*]

ABSTRACT

The primary cilium is a cellular compartment specialized for receipt of extracellular signals that is essential for development and homeostasis. Although intraciliary responses to engagement of ciliary receptors are well studied, fundamental questions remain about the mechanisms and molecules that transduce ciliary signals into responses in the cytoplasm. During fertilization in the bi-ciliated alga *Chlamydomonas reinhardtii*, ciliary adhesion between *plus* and *minus* gametes triggers an immediate ∼10-fold increase in cellular cAMP and consequent responses in the cytoplasm required for cell–cell fusion. Here, we identify a new participant in ciliary signaling, Gamete-Specific Protein Kinase (GSPK). GSPK is essential for the adhesion-induced cAMP increase and for rapid gamete fusion. The protein is in the cytoplasm, and the entire cellular complement responds to a signal from the cilium by becoming phosphorylated within 1 min after ciliary receptor engagement. Unlike all other cytoplasmic events in ciliary signaling, GSPK phosphorylation is not responsive to exogenously added cAMP. Thus, during ciliary signaling in *Chlamydomonas,* a cytoplasmic protein is required to rapidly interpret a still uncharacterized ciliary signal to generate a cytoplasmic response.

KEY WORDS: Ciliary signaling pathway, *Chlamydomonas*, Protein kinase, cAMP, Fertilization, Gamete fusion

INTRODUCTION

The primary cilium transduces cues from the extracellular milieu into cellular responses in the cytoplasm. In some ciliary signaling systems, changes in concentrations of cyclic nucleotides within cilia that are triggered by receptor activation lead to responses within the organelles that activate action potentials in the neuronal plasma membrane (vision and olfaction) (Dell'Orco et al., 2021; Dhallan et al., 1990; Nakamura, 2000), or delivery to the cytoplasm of an active transcription factor (the Hedgehog developmental pathway) (Bangs and Anderson, 2017; Nachury and Mick, 2019; Wen et al., 2010). In many others, including ciliary regulation of adipogenesis and ciliary regulation of glucagon and insulin secretion, cAMP diffusing from the cilium is a candidate carrier of cilium-to-cytoplasm information, but definitive signals are still unknown (Hilgendorf, 2021; Hilgendorf et al., 2019; Siljee et al., 2018; Wachten and Mick, 2021; Wu et al., 2021).

We are using ciliary adhesion-induced signaling during fertilization in the bi-ciliated, unicellular green alga *Chlamydomonas reinhardtii* (hereafter *Chlamydomonas*) as a model system to investigate mechanisms of cilium-to-cytoplasm communication. When *plus* and *minus* gametes encounter each other, their cilia adhere through the adhesion receptor SAG1 on *plus* cilia and SAD1 on *minus* cilia. SAG1–SAD1 engagement leads to an almost immediate ∼10-fold increase in total cellular cAMP, and consequent activation of an array of responses in the cell bodies that prepare the gametes for cell–cell fusion (Fig. 1A) (Pasquale and Goodenough, 1987; Pijst et al., 1984; Saito et al., 1993; Snell and Goodenough, 2009; Zhang et al., 1991). As with many metazoan systems, the mechanisms that couple ciliary signaling to cytoplasmic responses in *Chlamydomonas* are unknown. Here, we identify a protein kinase, Gamete-Specific Protein Kinase (GSPK), that is essential for the large, ciliary adhesion-induced increase in cellular cAMP. Surprisingly, GSPK is present in the cytoplasm and the entire cellular complement of the protein is phosphorylated within 1 min after SAG1–SAD1 engagement in the cilia. Moreover, even though all other cell body events triggered by ciliary adhesion can be induced in gametes of a single mating type by addition of a cell-permeable analog of cAMP, GSPK fails to be phosphorylated upon addition of the analog. Thus, GSPK is responsive to a non-cAMP-mediated signal generated by ciliary adhesion and central for transduction of ciliary adhesion into the large increase in cAMP required for fusion-essential cell body responses.

RESULTS AND DISCUSSION

To identify gamete-specific proteins that function during ciliary signaling, we tested for a fertilization phenotype in several *Chlamydomonas* CLiP library mutants that were annotated to contain mutations in genes that exhibit gamete-specific expression profiles (Fig. 1B) (Li et al., 2016; Ning et al., 2013). One mutant strain [hereafter termed *gspk*(−)] with a mutation in *Cre02.g104450* (which encodes GSPK) (Fig. S1A, Table S1), was strongly impaired in gamete fusion (Fig. 1C), as were two independent *gspk* CLiP mutant strains, *gspk-2* and *gspk-3* (Fig. 1C; Figs S1B,C, Table S1). Fusion between wild-type *plus* [WT(+)] gametes and *gspk*(−) gametes at 10 min after mixing was reduced over 50-fold compared to WT(+) and WT(−) gametes and increased slightly by 60 min (Fig. 1C). The fusion phenotype co-segregated with the genotype and was present in both *gspk*(+) and *gspk*(−) gametes (Fig. 1D; Fig. S1D). A separate CRISPR-generated (Greiner et al., 2017; Kelterborn et al., 2022) *gspk*(+) strain also exhibited the fusion phenotype (Fig. 1D; Fig. S2). As expected, gamete activation and cell–cell fusion by *gspk* mutants was rescued by introduction of a transgene encoding an epitope-tagged form of GSPK, *GSPK-HA*

[1]Department of Cell Biology and Molecular Genetics, University of Maryland, College Park, MD. [2]Experimental Biophysics, Institute for Biology, Humboldt-Universität zu Berlin, Berlin, Germany. [3]Charité – Universitätsmedizin Berlin, Institute of Translational Physiology, Berlin, Germany.

*Author for correspondence (wsnell1@umd.edu)

M.A., 0000-0002-4395-0589; W.J.S., 0000-0002-1659-6211

Handling Editor: Guangshuo Ou
Received 26 January 2022; Accepted 25 April 2022

Journal of Cell Science (2022) 135, jcs259814. doi:10.1242/jcs.259814

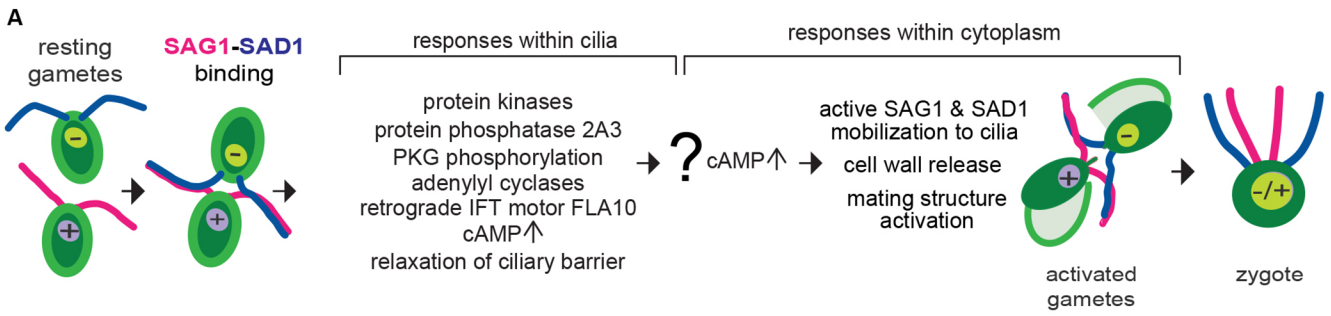

B

GeneID	Protein	Transcript abundance (RPKM) V-asynch	V-synch	mt- G	mt- G + db-cAMP	mt+ G	mt+ G + db-cAMP	Fusion phenotype
Cre02.g075700	RPL19 (ribosomal subunit)	1503	1694	1551	1907	1491	1536	-
Cre08.g374250	SAG1 (plus adhesion protein)	0	0	1	0	79	344	no fusion
Cre06.g255000	SAD1 (adhesion protein)	0	0	28	168	0	0	no fusion
Cre02.g086100	ATPase	22	12	7	918	3	2831	wt
Cre09.g395750	ATPase	2	1	1	2565	3	2342	wt
Cre04.g220850	ATPase	2	1	3	1444	4	666	wt
Cre07.g332950	SF-assemblin	14	2	77	1359	182	646	wt
Cre12.g532950	Glutamate receptor	1	0	26	1026	532	306	wt
Cre12.g537400	Aurora kinase	3	2	77	626	229	681	wt
Cre02.g107000	Protein kinase	3	2	48	188	75	81	wt
Cre04.g215700	Protein kinase	1	0	0	118	0	10	wt
Cre12.g556250	Septin 7	30	16	51	6	108	7	wt
Cre12.g510600	Protein kinase	4	2	13	74	23	38	wt
Cre02.g112500	Aurora Kinase	1	1	73	10	60	6	wt
Cre14.g625600	ATPase with PKD/REJ domain	0	0	4	1	69	52	wt
Cre02.g087750	Protein kinase	5	3	15	37	19	5	wt
Cre06.g287450	Protein kinase	1	1	16	30	8	6	wt
Cre02.g104450	Protein kinase (GSPK)	0	0	10	0	24	2	impaired
Cre16.g689300	Protein kinase	4	3	17	3	18	1	wt
Cre10.g435750	Protein kinase	0	1	0	0	5	1	wt

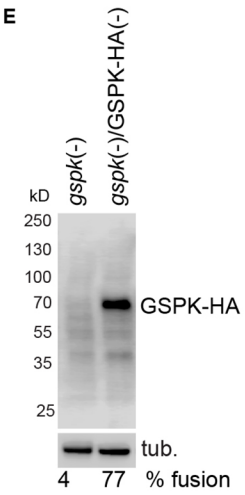

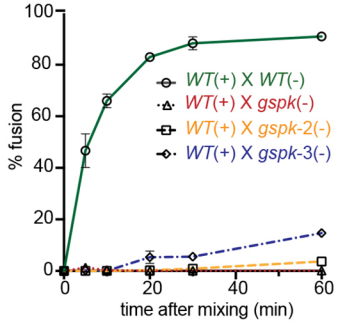

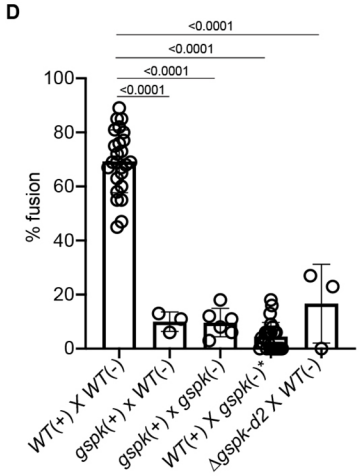

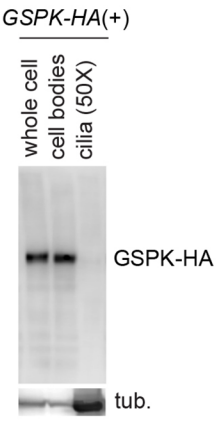

Fig. 1. GSPK is a gamete-specific cytoplasmic protein essential for cell–cell fusion in *Chlamydomonas*. (A) Graphic representation of fertilization in *Chlamydomonas*. (B) The *Cre02.g104450* insertion strain *LMJ.RY0402.138658* has a fusion phenotype. Transcript abundance in asynchronized (V-asynch) and synchronized (V-synch) vegetative cells, naive *minus* (mt– G) and *plus* (mt+ G) gametes, and db-cAMP-activated *minus* (mt– G, db-cAMP) and *plus* (mt+ G, db-cAMP) gametes represented by median reads per kilobase per million mapped reads [RPKM; data are from Ning et al. (2013)]. *RPL19* is a housekeeping gene. (C) Quantification of fusion of WT(+) gametes with WT(–) and three different CLiP *gspk*(–) mutants. Values are mean±s.d. from three independent experiments. (D) Quantification (mean±s.d.) of gamete fusion of WT(+) with WT(–) (n=25 experiments); of *gspk*(+) mutant progeny generated from a cross between *gspk*(–) and WT(+) (n=3); *gspk*(+) with *gspk*(–) (n=7); of WT(+) with *gspk**(–) mutant progeny generated from a cross between *gspk*(+) and WT(–) (n=25); and of CRISPR-generated Δ*gspk-d2*(+) with WT(–) (n=3). *P*-values above the groups compared are by an unpaired two-tailed Student's *t*-test. (E) Expression of GSPK–HA in *gspk*(–) gametes rescues fusion. Anti-HA immunoblot of *gspk*(–) and *GSPK-HA*-rescued *gspk*(–) gametes. The percentage of fusion at 10 min is shown below the blot (n=3). (F) GSPK–HA expression is gamete specific. Anti-HA immunoblot of *gspk*/*GSPK-HA*(+) vegetative cells (V), naive gametes (G), and gametes activated by incubation for 1 h in db-cAMP buffer (G-A). (G) GSPK fractionates with cell bodies. Anti-HA immunoblot of whole cells, cell bodies, and isolated cilia of *gspk*/*GSPK-HA*(+) gametes. Each lane contain 3 µg of protein, which for cilia represents ∼50 cell equivalents. The lower panels in E–G show tubulin (tub.) as a loading control. Blots shown represent at least three repeats.

Journal of Cell Science (2022) 135, jcs259814. doi:10.1242/jcs.259814

(Fig. 1E; Fig. S3). Consistent with the downregulation of GSPK transcripts during prolonged dibutyryl (db)-cAMP-induced gamete activation, the levels of the GSPK–HA protein were also substantially reduced after prolonged activation (Fig. 1F). Cell fractionation and immunoblotting indicated that GSPK was present in cell bodies, with little if any detectable in cilia (Fig. 1G). Finally, consistent with the published annotation (Goodstein et al., 2012), analysis of the GSPK protein sequence indicated that it indeed possessed all of the canonical protein kinase subdomains, with highest similarity to mixed lineage protein kinases (Fig. S4).

Cell body responses to ciliary adhesion are severely impaired in *gspk* mutant gametes

Vegetative *gspk* cells and naive *gspk* gametes were indistinguishable from WT in morphology, growth, and motility (data not shown), and the mutant gametes underwent initial ciliary adhesion to nearly the same extent as WT (Fig. 2A). We found, however, that *gspk* gametes were impaired in ciliary adhesion-induced cytoplasmic responses required for cell–cell fusion. Cell wall release was reduced nearly 3-fold and mating structure activation in *gspk*(+) gametes was almost completely blocked (Fig. 2B,C). Addition of db-cAMP to *gspk* gametes induced cell wall loss and mating structure activation similarly to WT gametes (Fig. 2B,C; Fig. S4) and also rescued fusion (Fig. 2D), indicating that the *gspk* mutants were capable of responding to the second messenger. Notably, and similar to earlier studies (Pasquale and Goodenough, 1987; Saito et al., 1993; Zhang and Snell, 1994), cAMP levels increased over 10-fold within 1–2 min after mixing WT(+) with fusion-defective *hap2*(−) gametes, but the increase was less than 2-fold at 1 min after *gspk*(−) and *gspk*(+) gametes were mixed. Furthermore, unlike in the control mixture, the (slight) cAMP increase was not sustained in the mutants (Fig. 2E). Thus, this cytoplasmic protein is required to transduce SAG1–SAD1 interactions in the cilia into responses in the cytoplasm, and GSPK function is required within the first minute after the ciliary signal is initiated.

Ciliary responses to ciliary adhesion are intact in the *gspk* mutants

We assessed whether intra-ciliary responses to ciliary receptor engagement were intact in the *gspk* mutants. Consistent with previous results (Wang et al., 2006; Wang and Snell, 2003), phosphorylation of the previously identified ciliary cGMP-dependent protein kinase (PKG) in isolated cilia was detected in samples of cilia isolated from adhering, but not non-adhering, WT gametes. Moreover, it was similarly phosphorylated in cilia samples isolated from adhering *gspk* gametes (Fig. 3A). Thus, GSPK is dispensable for this intraciliary biochemical response to SAG1–SAD1.

We also examined whether the previously described barrier to SAG1 entry onto cilia was removed during SAG1–SAD1 interactions between *gspk* mutant gametes. In naive gametes, only a small portion of total cellular SAG1 is present in cilia, and the remainder is in a non-exchanging, inactive pool on the surface of the cell body plasma membrane (Belzile et al., 2013; Cao et al., 2015; Hunnicutt et al., 1990; Musgrave et al., 1986; Ranjan et al., 2019). During ciliary adhesion, however, the ciliary barrier is relaxed to allow SAG1 entry. Moreover, the ciliary adhesion-induced increase in cellular cAMP induces rapid recruitment of SAG1 from an inactive pool on the plasma membrane onto the ciliary membrane as part of a mechanism to support and enhance ciliary adhesion (Cao et al., 2015; Goodenough, 1989; Hunnicutt et al., 1990; Ranjan et al., 2019; Saito et al., 1985). Immunoblotting of samples taken after mixing *gspk/SAG1-HA*(+) gametes and WT *SAG1-HA*(+) gametes with fusion-defective *hap2*(−) gametes showed that at 10 min after mixing, SAG1–HA had moved into the cilia of both the WT gamete mixtures and those of the *gspk* gametes (Fig. 2B). Thus, GSPK is dispensable for this second intraciliary response to ciliary adhesion, removal of the ciliary barrier.

Notably, though, at 45 min after mixing, SAG1–HA had continued to increase in the cilia of the WT gametes (Fig. 3B), but it had decreased in the cilia of the *gspk/SAG1-HA* gametes, even though levels of SAG1–HA remained high in both sets of cell bodies (Fig. 3B). Thus, consistent with the requirement for GSPK for the large increase in cellular cAMP, active SAG1 mobilization from the cell body and enrichment in the cilia also requires GSPK. Reflecting the loss of SAG1 from the *gspk* cilia, the clusters of adhering *gspk plus* and *minus* gametes that had initially formed had disassembled by 45 min, although the clusters had become even larger in mixtures of WT(+) and *hap2*(−) gametes (Fig. 3C). Taken together, these results indicate that the immediate intra-ciliary responses to ciliary adhesion are independent of GSPK, but the cytoplasmic responses to ciliary adhesion, including mobilization of cell body SAG1 to the cilia, depend on GSPK.

Ciliary adhesion, but not addition of db-cAMP, triggers rapid phosphorylation of the entire cellular complement of GSPK

Because most protein kinases undergo changes in phosphorylation state at steps in the signaling pathways in which they function, we assessed GSPK phosphorylation state in naive gametes, in gametes undergoing ciliary adhesion, and in non-adhering gametes of a single mating type undergoing activation induced by db-cAMP. SDS-PAGE and immunoblotting of lysates of naive GS*PK-HA*(−) gametes before and after incubation with the protein de-phosphorylating enzyme λ-phosphatase showed that the phosphatase incubation led to a shift in migration of GSPK. Thus, GSPK was basally phosphorylated (Fig. 4A) in naive gametes. Moreover, when *GSPK-HA*(+) gametes were mixed with *hap2*(−) gametes, GSPK–HA became phosphorylated within 1 min after mixing, and, remarkably, the entire cellular complement of GSPK–HA underwent this ciliary adhesion-triggered phosphorylation (Fig. 4B). Notably, experimentally activating *GSPK-HA*(+) gametes alone with db-cAMP failed to alter GSPK-HA phosphorylation state, indicating that phosphorylation is upstream of the ciliary adhesion-induced cAMP increase.

Conclusion

Our studies have uncovered a new participant in ciliary signaling in *Chlamydomonas* and showed that it functions at a previously unrecognized step in the ciliary signaling pathway. GSPK is not required for responses within the cilia to ciliary adhesion – phosphorylation of a ciliary PKG (Wang et al., 2006; Wang and Snell, 2003) and relaxation of the ciliary barrier to entry of SAG1 (Belzile et al., 2013; Pan and Snell, 2002) – but it is required for the adhesion-induced increase in cellular cAMP required for gamete activation. Most importantly, GSPK is a cytoplasmic protein and responds to ciliary signaling within 1 min by becoming phosphorylated. Unlike all other characterized ciliary adhesion-induced cytoplasmic responses, however, including cell wall loss, mating structure activation, and sustained cell body mobilization and ciliary enrichment of SAG1, the change in phosphorylation state of GSPK fails to occur upon experimental gamete activation induced by exogenously added cAMP. Our findings are at odds with previous suggestions that cAMP diffusing from cilia during ciliary adhesion is responsible for triggering the subsequent large increase

Journal of Cell Science (2022) 135, jcs259814. doi:10.1242/jcs.259814

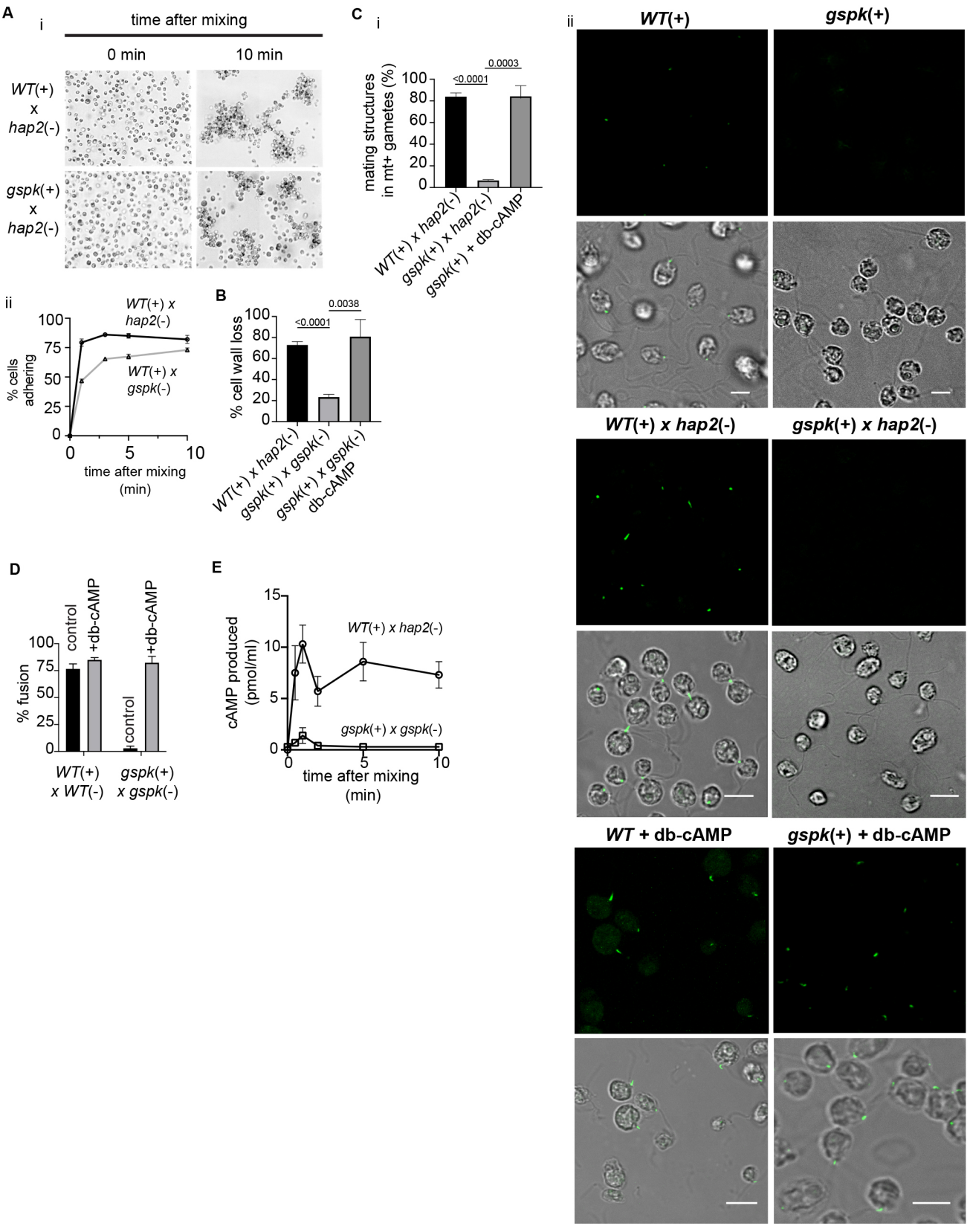

Fig. 2. See next page for legend.

in cell body cAMP and gamete activation (Pasquale and Goodenough, 1987; Pijst et al., 1984; Saito et al., 1993; Zhang and Snell, 1994; Zhang et al., 1991), and indicate that signaling within cilia triggers transmittance of a still unidentified signal to the cytoplasm that regulates GSPK function. A recent report showing that generation of ciliary, but not cytoplasmic cAMP, regulated the

Journal of Cell Science (2022) 135, jcs259814. doi:10.1242/jcs.259814

Fig. 2. Ciliary adhesion between *gspk* mutants fails to trigger the large sustained increase in cellular cAMP, and cell body responses are impaired in *gspk* mutants, but restored by db-cAMP buffer. (A) Ciliary adhesion is similar in *gspk*(+) and WT(+) gametes. (Ai) Differential interference contrast (DIC) micrographs of mixtures of the indicated gametes. Because the *gspk*(+) gametes are defective in fusion, fusion-defective *hap2*(−) gametes lacking the HAP2 fusion protein were used as controls instead of WT(−) gametes. (Aii) Electronic particle counter quantification of adhesion in the indicated samples. (B) *gspk* gametes are impaired in cell wall loss and mating structure activation. Quantification of cell wall loss after mixing WT(+) and *hap2*(−) gametes and *gspk*(+) and *gspk*(−) gametes in the absence and presence of db-cAMP buffer. (C) Actin-filled fertilization tubules fail to form in adhering *gspk*(+) gametes. Quantification (Ci) and fluorescence images (Cii) of mating structures in *plus* gametes in the 50:50 mixtures of WT(+) and *hap2*(−) gametes and *gspk*(+) and *hap2*(−) gametes at 10 min after mixing and in samples of *gspk*(+) gametes incubated with db-cAMP buffer for 30 min. Scale bars: 10 µm. (D) Fusion of *gspk* gametes is rescued by db-cAMP. Quantification of gamete fusion in the indicated mixtures in the presence or absence of db-cAMP. (E) The ciliary adhesion-induced increase in cAMP is impaired in *gspk* gametes. cAMP concentrations were determined at the indicated times after mixing WT(+) and WT(−) gametes and *gspk(+)* and *gspk*(−) gametes. *P*-values shown for B,C are from comparisons of means by unpaired two-tailed Student's *t*-test. Quantitative results are shown as mean±s.d. Data represent values from eight independent experiments.

Hedgehog pathway in vertebrate cells (Truong et al., 2021) also indicates that ciliary and cytoplasmic concentrations of cAMP are tightly regulated. And, the recent report that binding of melanin-concentrating hormone to its ciliary receptor on cultured mouse hippocampal neurons triggers phosphorylation of the extracellular signal-related kinases Erk1/2, detectable within 3 min after hormone addition (Hsiao et al., 2021), suggests that cytoplasmic protein kinases also participate at very early steps in vertebrate ciliary signaling.

In future studies, it will be important to test for relationships between GSPK and the three other proteins previously shown to participate in gamete-activated ciliary signaling downstream of SAG1–SAD1 interactions – the ciliary PKG (Wang et al., 2006; Wang and Snell, 2003), a protein phosphatase 2A catalytic subunit (PP2A3) (Lin et al., 2013), and the anterograde intraflagellar transport (IFT) kinesin 2 family member FLA10 (Pan and Snell, 2002). Because all three are present in cilia, and because FLA10 is required for intraciliary phosphorylation of PKG, all 3 might function upstream of GSPK. It will also be important to learn whether the adhesion-induced phosphorylation of GSPK is essential for its function during gamete activation and whether its protein kinase activity is required to induce the increase in cellular cAMP through as yet unidentified adenylyl cyclases or

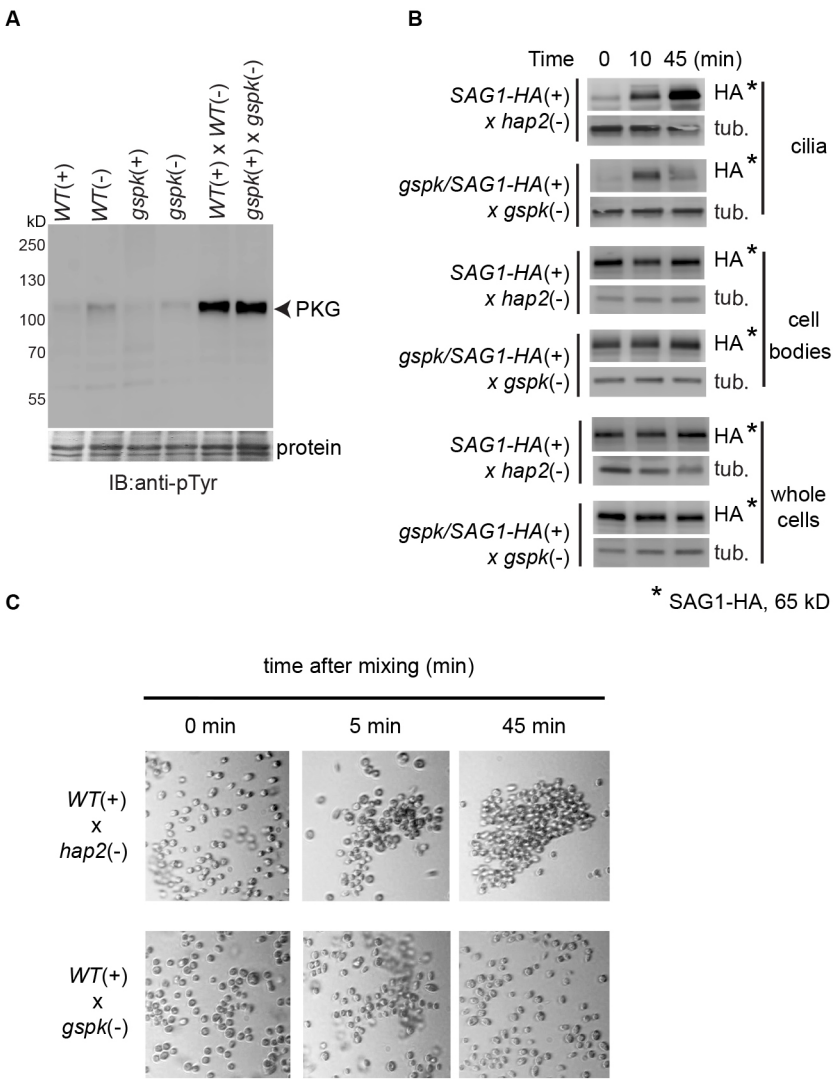

Fig. 3. Intraciliary responses to SAG1–SAD1 interactions, namely, PKG phosphorylation and removal of the ciliary barrier, are intact in *gspk* mutants. (A) Ciliary adhesion in *gspk* gametes induces phosphorylation of cGMP-dependent protein kinase (PKG) similarly to in wild-type gametes. PKG phosphorylation assessed in samples of cilia isolated from WT(+), WT(−), *gspk*(+) and *gspk*(−) gametes and the indicated samples of gametes that had been mixed for 10 min. Ponceau protein staining is shown as a loading control. (B) As in WT(+) gametes, the ciliary barrier to passive movement of SAG1 from the cell body to the cilium is removed during ciliary adhesion of *gspk* mutants. Anti-HA immunoblots of whole cells, cell bodies, and cilia from the indicated samples harvested 0, 10 and 45 min after WT(+) and *gspk*(+) gametes expressing SAG1-HA were separately mixed with *gspk*(−) gametes. The lower panel is a tubulin (tub.) loading control. 3 µg of protein (~50 cell equivalents of cilia compared to cell bodies and whole cells) were loaded in each lane. (C) The reduction in ciliary SAG1–HA in the *gspk*(+) gametes at 45 min is reflected in loss of ciliary adhesion and the consequent disassembly of gamete clusters. DIC images taken at the indicated times after mixing WT(+) gametes with *hap2*(−) gametes and WT(+) gametes with *gspk*(−) gametes. Images shown represent three repeats.

Journal of Cell Science (2022) 135, jcs259814. doi:10.1242/jcs.259814

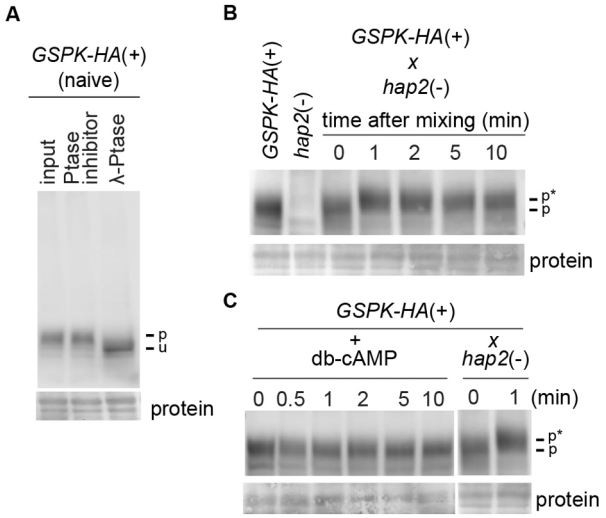

Fig. 4. GSPK phosphorylation state is altered within 1 min after initiation of ciliary adhesion, but is unchanged by incubation in db-cAMP. (A) GSPK–HA is basally phosphorylated in naive gametes. Anti-HA immunoblot of lysates of *gspk*/*GSPK-HA*(+) naive gametes that had been incubated with λ-phosphatase with or without a phosphatase inhibitor. (B) The entire cellular complement of GSPK–HA is phosphorylated within 1 min after initiation of ciliary adhesion. Anti-HA immunoblots of *GSPK-HA*(+) gametes at the indicated times after ciliary adhesion was initiated by mixing with *hap2*(−) gametes. (C) Activation of gametes with db-cAMP buffer fails to induce phosphorylation of GSPK-HA. Anti-HA immunoblots of *gspk*/*GSPK-HA*(+) gametes at the indicated times after gamete activation was induced by incubation with db-cAMP buffer. Cell wall loss was over 80% at 10 min, confirming gamete activation. The two lanes on the right showing non-adhering and adhering *gspk*/*GSPK-HA*(+) gametes (from B), are shown for comparison. For all the blots, Ponceau protein staining is shown as loading controls. Labels on the right indicate GSPK–HA that is unphosphorylated (u), basally phosphorylated (p), or additionally phosphorylated (p*). Blots shown represent three repeats.

phosphodiesterases. Perhaps of even more importance, though, will be to use this system to investigate the undefined signal transmitted from adhering cilia to the cytoplasm and the mechanism of its transport.

MATERIALS AND METHODS

Experimental model

Chlamydomonas reinhardtii wild-type strains *21gr* (mating type *plus*; mt+; CC-1690; designated WT(+), *CMJ030* (mating type *minus*; mt−; CC-5325; designated WT(−), *hap2 (40D4;* CC5281*)* and *SAG1-HA* strains used in this study were grown in liquid tris-acetate phosphate medium (TAP) medium containing trace metals at 22°C with aeration, or on 1.5% TAP agar plates (Wang and Snell, 2003). Gametogenesis was induced by transferring vegetatively growing cells into nitrogen-free medium (M-N) along with continuous light incubation overnight with aeration or agitation (Snell and Roseman, 1979). *Chlamydomonas* CLiP library mutants (Li et al., 2019) were obtained from the *Chlamydomonas* Resource Center. Genomic DNA was isolated from single colonies using Clontech plant genomic DNA isolation reagent, and the insertion site of the CIB1 cassette in each mutant was verified by PCR using the primers listed in Table S1. Cell numbers were determined with a hemocytometer.

Plasmid construction, transformation and genetic crosses

To prepare a plasmid containing a *GSPK* gene encoding an HA-tagged GSPK protein, a gene fragment of 8769 bp that included the full-length *GSPK* gene sequence (7272 bp) and an additional 850 bp 5′ to the annotated transcription start site predicted to include the endogenous promoter and an additional 647 bp 3′ to the stop codon was amplified from DNA of BAC clone 34G21 by PCR using primers possessing *Xho1* and *Not1* restriction sites at the 5′ and 3′ ends, respectively. The PCR product was cloned into a paromomycin resistance vector, *pChlamiRNA3int* (*Chlamydomonas* Resource Center) in between *Xho1* and *Not1* restriction sites by In-fusion HD EcoDry cloning plus kit. A gene fragment encoding three copies of the 9-amino-acid HA epitope followed by *EcoR1* and *XbaI* restriction sites was inserted using QuikChange II XL Site-Directed Mutagenesis Kit (Table S2). The resulting *GSPK-HA* transgene plasmid (13,468 bp) was verified by sequencing. For *Chlamydomonas* transformation, purified *BspH1*-linearized *pGSPK-HA* was electroporated into *21gr* mt+ and *CC-5325* mt− strains (Shimogawara et al., 1998). Transformants that grew on TAP-paromomycin plates were picked into 96-well plates and screened for *GSPK-HA* by PCR using primer sets P1_Fwd and P2_Rev to confirm N-terminal end, P3_Fwd and P4_Rev to confirm the presence of in-frame HA-tag and P5_Fwd and P6_Rev to confirm the C-terminal end as shown in Fig. S2. PCR-positive transformants were screened for GSPK expression by immunoblotting. *gspk*(−) strains expressing GSPK–HA were obtained as progeny from crosses between *GSPK-HA*(+) cells and *gspk*(−) cells. Colonies were screened for mating type by bioassays and for the presence of the insertion cassette in the *GSPK* gene by PCR using primers listed in Table S1, followed by further selection for GSPK–HA expression by immunoblotting.

Protein determination, SDS-PAGE and immunoblotting

Protein concentrations were determined with the Bradford assay. For immunoblotting, samples were separated by SDS-PAGE on 4–12% SDS-MOPS gradient gels and transferred onto PVDF membranes as described previously (Belzile et al., 2013; Cao et al., 2015). Membranes were blocked by incubation in 3% fat-free dried milk for 1 h followed by 1 h of incubation in the primary antibody. Membranes were washed three times for 10 min with Tris-buffered saline with 0.1% Tween 20 (TBST) followed by incubation with secondary antibody. After three TBST washes and incubation in the chemiluminescent substrate, fluorescence signals were captured on a C-Digit blot scanner. Antibodies were rat anti-HA (1:3000 dilution; Roche, cat. no. 11867423001), mouse anti-α-tubulin (1:5000 dilution; Sigma, cat. no. T1026), goat anti-rat IgG HRP (1:5000 dilution; Merck, cat. no. AP136A), and goat anti-mouse-IgG HRP (1:5000 dilution; Sigma, cat. no. A9917).

Gamete activation, cell fractionation and PKG phosphorylation assay

For gamete activation, *plus* and *minus* gametes were mixed together or gametes of single mating types were incubated in M-N containing 15 mM db-cAMP and 150 µM papaverine (db-cAMP buffer) (Pasquale and Goodenough, 1987). Ciliary adhesion was quantified using an electronic particle counter (Snell and Moore, 1980; Snell and Roseman, 1979). Cell fractionation and assays for cell wall loss and gamete fusion were as described previously (Liu et al., 2008; Snell, 1982; Wang and Snell, 2003). Phosphorylation of PKG was assayed *in vitro* using a protein tyrosine kinase (PTK) assay (Wang and Snell, 2003). 20 µl of whole cilia (~3 µg/µl protein) in 5% sucrose, 20 mM HEPES buffer were mixed with 20 µl of 2× PTK buffer (20 mM HEPES, pH 7.2, 10 mM $MgCl_2$, 2 mM dithiothreitol, 1 mM EDTA, 50 mM KCl, 2 mM ATP, 0.2% Nonidet P-40, 0.4 mM orthovanadate, 20 mM β-glycerolphosphate, and 2% Sigma plant protease inhibitor cocktail) in the presence of ATP for 10 min and the phosphorylated form of PKG was detected by use of 4–20% gradient SDS-PAGE gels and immunoblotting using anti-phospho-tyrosine antibody (anti-p-Tyr; 1:1000 dilution; Sigma, cat. no. 05-321).

GSPK phosphorylation and λ-phosphatase treatment

GSPK phosphorylation in lysates of naive, adhering or db-cAMP-activated gametes was assessed by changes in migration in SDS-PAGE and immunoblotting. Samples were prepared by addition of 4× SDS-PAGE sample buffer followed by immediate boiling. For phosphatase treatment, 2×10^7 cells/ml in 1 ml in HEMDK buffer were briefly sonicated and 31 µl cell lysate, 1 µl λ-phosphatase (NEB, 400,000 U/µl), and 8 µl of phosphatase reaction buffer were incubated at 30°C for 30 min. Reactions

were terminated by adding 40 µl of 4×SDS sample buffer followed by boiling. As controls, samples were incubated in the presence of a phosphatase inhibitor cocktail (Sigma).

cAMP ELISA assay

cAMP amounts in adhering wild-type and *GSPK* mutant gametes were quantified by use of a cAMP Elisa kit. Equal numbers (100 µl, 2×10^7 cells/ml in M-N) of the WT and *gspk plus* and *minus* gametes were separately mixed in 1.5 ml Eppendorf tubes to initiate ciliary adhesion, and at the times indicated the cells were harvested by centrifugation (6350 ***g***; 4°C) and flash-frozen in liquid nitrogen. For assays, samples were resuspended in 100 µl of 0.1 M HCl and incubated at room temperature for 10 min followed by clarification by centrifugation (20,000 ***g***; 4°C). Supernatants were transferred to fresh tubes for use in the assay, which was performed using the acetylation protocol according to the manufacturer's instructions. Absorbances at 405 nm of standards and experimental samples were determined using a microplate reader. Results shown are from six independent experiments and are plotted as pmol/ml cAMP produced in the WT and *gspk* mutant mixtures.

Determination of mating structure activation

As described previously (Wilson et al., 1997), samples (~200 µl, 5×10^6 cells/ml) in M-N were seeded on coverslips coated with poly-L-lysine for 5 min followed by fixation with 4% paraformaldehyde solution freshly made in 10 mM HEPES, pH 7.4. Coverslips were washed with PBS for 3 min, immersed for 6 min in 80% acetone, 30 mM NaCl and 2 mM sodium phosphate buffer, pH 7.0, at −20°C, followed by immersion in 100% −20°C acetone 6 min. Filamentous actin in the fertilization tubules was visualized by staining with Alexa Flour 488–Phalloidin (Thermo Fisher Scientific, cat. no. A12379) for 15 min in the dark (Craig et al., 2019), followed by a 5-min PBS wash. Coverslips mounted on slides using ProLongTM Gold antifading agent were examined by a Hyd detector-equipped Leica TCS SP5 confocal microscope (1.4 numerical aperture, 63× oil immersion objective). *Z*-series images were summed to produce a projected image using Leica LAS X and cropped in Adobe Systems (USA) Illustrator.

Bioinformatic analysis and statistical analysis

Protein sequences were aligned with ClustalW, and the percentages of positions with identical or identical plus similar amino acid positions were calculated using BioEdit 7.2 software with a threshold of 75%. JPred4 was used to predict secondary structure (Drozdetskiy et al., 2015). N-terminal myristoylation sites were predicted using NMT – The MYR Predictor (Maurer-Stroh et al., 2002). All quantitative data represent at least three independent sets of experiments. Statistical significance of differences between groups was assessed by unpaired two-tailed Student's *t*-test. Data were analyzed using GraphPad Prism 9. All experiments were performed three to six times.

For the reagents used and their identifier numbers, please refer Table S3.

Acknowledgements

We are grateful to Dr Melanie Cobb of UT Southwestern Medical School, Dallas, TX and Dr Caren Chang, University of Maryland, College Park, MD for insightful discussions, our laboratory colleagues, Drs Jennifer Pinello and Jun Zhang for their constructive insights, and Amy Beaven and the CBMG Imaging Core Facility for use of the Leica TCS SP5 confocal microscope.

Competing interests

The authors declare no competing or financial interests.

Author contributions

Conceptualization: M.A., W.J.S.; Methodology: M.A., P.R., S.K., P.H., W.J.S.; Validation: M.A.; Formal analysis: M.A.; Resources: W.J.S.; Data curation: M.A., P.R.; Writing - original draft: M.A., W.J.S.; Writing - review & editing: M.A., P.R., S.K., P.H., W.J.S.; Visualization: M.A.; Supervision: W.J.S.; Funding acquisition: W.J.S.

Funding

This work was supported by National Institutes of Health grant GM122565 to W.J.S. Deposited in PMC for release after 12 months.

Peer review history

The peer review history is available online at https://journals.biologists.com/jcs/article-lookup/doi/10.1242/jcs.259814.

References

Bangs, F. and Anderson, K. V. (2017). Primary cilia and mammalian hedgehog signaling. *Cold Spring Harb. Perspect Biol.* **9**, a028175. doi:10.1101/cshperspect.a028175

Belzile, O., Hernandez-Lara, C. I., Wang, Q. and Snell, W. J. (2013). Regulated membrane protein entry into flagella is facilitated by cytoplasmic microtubules and does not require IFT. *Curr. Biol.* **23**, 1460-1465. doi:10.1016/j.cub.2013.06.025

Cao, M., Ning, J., Hernandez-Lara, C. I., Belzile, O., Wang, Q., Dutcher, S. K., Liu, Y. and Snell, W. J. (2015). Uni-directional ciliary membrane protein trafficking by a cytoplasmic retrograde IFT motor and ciliary ectosome shedding. *eLife* **4**, e05242. doi:10.7554/eLife.05242.010

Craig, E. W., Mueller, D. M., Bigge, B. M., Schaffer, M., Engel, B. D. and Avasthi, P. (2019). The elusive actin cytoskeleton of a green alga expressing both conventional and divergent actins. *Mol. Biol. Cell* **30**, 2827-2837. doi:10.1091/mbc.E19-03-0141

Dell'Orco, D., Koch, K. W. and Rispoli, G. (2021). Where vision begins. *Pflugers Arch.* **473**, 1333-1337. doi:10.1007/s00424-021-02605-3

Dhallan, R. S., Yau, K.-W., Schrader, K. A. and Reed, R. R. (1990). Primary structure and functional expression of a cyclic nucleotide-activated channel from olfactory neurons. *Nature* **347**, 184-187. doi:10.1038/347184a0

Drozdetskiy, A., Cole, C., Procter, J. and Barton, G. J. (2015). JPred4: a protein secondary structure prediction server. *Nucleic Acids Res.* **43**, W389-W394. doi:10.1093/nar/gkv332

Goodenough, U. W. (1989). Cyclic AMP enhances the sexual agglutinability of *Chlamydomonas* flagella. *J. Cell Biol.* **109**, 247-252. doi:10.1083/jcb.109.1.247

Goodstein, D. M., Shu, S., Howson, R., Neupane, R., Hayes, R. D., Fazo, J., Mitros, T., Dirks, W., Hellsten, U., Putnam, N. et al. (2012). Phytozome: a comparative platform for green plant genomics. *Nucleic Acids Res.* **40**, D1178-D1186. doi:10.1093/nar/gkr944

Greiner, A., Kelterborn, S., Evers, H., Kreimer, G., Sizova, I. and Hegemann, P. (2017). Targeting of photoreceptor genes in *Chlamydomonas reinhardtii* via zinc-finger nucleases and CRISPR/Cas9. *Plant Cell* **29**, 2498-2518. doi:10.1105/tpc.17.00659

Hilgendorf, K. I. (2021). Primary cilia are critical regulators of white adipose tissue expansion. *Front. Physiol.* **12**, 769367. doi:10.3389/fphys.2021.769367

Hilgendorf, K. I., Johnson, C. T., Mezger, A., Rice, S. L., Norris, A. M., Demeter, J., Greenleaf, W. J., Reiter, J. F., Kopinke, D. and Jackson, P. K. (2019). Omega-3 fatty acids activate ciliary FFAR4 to control adipogenesis. *Cell* **179**, 1289-1305.e21. doi:10.1016/j.cell.2019.11.005

Hsiao, Y. C., Muñoz-Estrada, J., Tuz, K. and Ferland, R. J. (2021). The transition zone protein AHI1 regulates neuronal ciliary trafficking of MCHR1 and its downstream signaling pathway. *J. Neurosci.* **41**, 3932-3943. doi:10.1523/JNEUROSCI.2993-20.2021

Hunnicutt, G. R., Kosfiszer, M. G. and Snell, W. J. (1990). Cell body and flagellar agglutinins in *Chlamydomonas reinhardtii*: the cell body plasma membrane is a reservoir for agglutinins whose migration to the flagella is regulated by a functional barrier. *J. Cell Biol.* **111**, 1605-1616. doi:10.1083/jcb.111.4.1605

Kelterborn, S., Boehning, F., Sizova, I., Baidukova, O., Evers, H. and Hegemann, P. (2022). Gene editing in green alga *Chlamydomonas reinhardtii* via CRISPR-Cas9 ribonucleoproteins. *Methods Mol. Biol.* **2379**, 45-65. doi:10.1007/978-1-0716-1791-5_3

Li, X., Zhang, R., Patena, W., Gang, S. S., Blum, S. R., Ivanova, N., Yue, R., Robertson, J. M., Lefebvre, P. A., Fitz-Gibbon, S. T. et al. (2016). An indexed, mapped mutant library enables reverse genetics studies of biological processes in *Chlamydomonas reinhardtii*. *Plant Cell* **28**, 367-387. doi:10.1105/tpc.15.00465

Li, X., Patena, W., Fauser, F., Jinkerson, R. E., Saroussi, S., Meyer, M. T., Ivanova, N., Robertson, J. M., Yue, R., Zhang, R. et al. (2019). A genome-wide algal mutant library and functional screen identifies genes required for eukaryotic photosynthesis. *Nat. Genet.* **51**, 627-635. doi:10.1038/s41588-019-0370-6

Lin, H., Miller, M. L., Granas, D. M. and Dutcher, S. K. (2013). Whole genome sequencing identifies a deletion in protein phosphatase 2A that affects its stability and localization in *Chlamydomonas reinhardtii*. *PLoS Genet.* **9**, e1003841. doi:10.1371/journal.pgen.1003841

Liu, Y., Tewari, R., Ning, J., Blagborough, A. M., Garbom, S., Pei, J., Grishin, N. V., Steele, R. E., Sinden, R. E., Snell, W. J. et al. (2008). The conserved plant sterility gene HAP2 functions after attachment of fusogenic membranes in *Chlamydomonas* and *Plasmodium* gametes. *Genes Dev.* **22**, 1051-1068. doi:10.1101/gad.1656508

Maurer-Stroh, S., Eisenhaber, B. and Eisenhaber, F. (2002). N-terminal N-myristoylation of proteins: prediction of substrate proteins from amino acid sequence[1]. *J. Mol. Biol.* **317**, 541-557. doi:10.1006/jmbi.2002.5426

Musgrave, A., de Wildt, P., van Etten, I., Pijst, H., Scholma, C., Kooijman, R., Homan, W. and van den Ende, H. (1986). Evidence for a functional membrane barrier in the transition zone between the flagellum and cell body of *Chlamydomonas eugametos* gametes. *Planta* **167**, 544-553. doi:10.1007/BF00391231

Nachury, M. V. and Mick, D. U. (2019). Establishing and regulating the composition of cilia for signal transduction. *Nat. Rev. Mol. Cell Biol.* **20**, 389-405. doi:10.1038/s41580-019-0116-4

Nakamura, T. (2000). Cellular and molecular constituents of olfactory sensation in vertebrates. *Comp. Biochem. Physiol. A Mol. Integr. Physiol.* **126**, 17-32. doi:10.1016/S1095-6433(00)00191-4

Ning, J., Otto, T. D., Pfander, C., Schwach, F., Brochet, M., Bushell, E., Goulding, D., Sanders, M., Lefebvre, P. A., Pei, J. et al. (2013). Comparative genomics in *Chlamydomonas* and *Plasmodium* identifies an ancient nuclear envelope protein family essential for sexual reproduction in protists, fungi, plants, and vertebrates. *Genes Dev.* **27**, 1198-1215. doi:10.1101/gad.212746.112

Pan, J. and Snell, W. J. (2002). Kinesin-II is required for flagellar sensory transduction during fertilization in *Chlamydomonas*. *Mol. Biol. Cell* **13**, 1417-1426. doi:10.1091/mbc.01-11-0531

Pasquale, S. M. and Goodenough, U. W. (1987). Cyclic AMP functions as a primary sexual signal in gametes of *Chlamydomonas reinhardtii*. *J. Cell Biol.* **105**, 2279-2292. doi:10.1083/jcb.105.5.2279

Pijst, H. L. A., van Driel, R., Janssens, P. M. W., Musgrave, A. and van den Ende, H. (1984). Cyclic AMP is involved in sexual reproduction of *Chlamydomonas eugametos*. *FEBS Lett.* **174**, 132-136. doi:10.1016/0014-5793(84)81091-1

Ranjan, P., Awasthi, M. and Snell, W. J. (2019). Transient internalization and microtubule-dependent trafficking of a ciliary signaling receptor from the plasma membrane to the cilium. *Curr. Biol.* **29**, 2942-2947.e2. doi:10.1016/j.cub.2019.07.022

Saito, T., Tsubo, Y. and Matsuda, Y. (1985). Synthesis and turnover of cell body-agglutinin as a pool of flagellar surface-agglutinin in *Chlamydomonas reinhardtii* gamete. *Arch. Microbiol.* **142**, 207-210. doi:10.1007/BF00693391

Saito, T., Small, L. and Goodenough, U. W. (1993). Activation of adenylyl cyclase in *Chlamydomonas reinhardtii* by adhesion and by heat. *J. Cell Biol.* **122**, 137-147. doi:10.1083/jcb.122.1.137

Shimogawara, K., Fujiwara, S., Grossman, A. and Usuda, H. (1998). High-efficiency transformation of *Chlamydomonas reinhardtii* by electroporation. *Genetics* **148**, 1821-1828. doi:10.1093/genetics/148.4.1821

Siljee, J. E., Wang, Y., Bernard, A. A., Ersoy, B. A., Zhang, S., Marley, A., Von Zastrow, M., Reiter, J. F. and Vaisse, C. (2018). Subcellular localization of MC4R with ADCY3 at neuronal primary cilia underlies a common pathway for genetic predisposition to obesity. *Nat. Genet.* **50**, 180-185. doi:10.1038/s41588-017-0020-9

Snell, W. J. (1982). Study of the release of cell wall degrading enzymes during adhesion of *Chlamydomonas* gametes. *Exp. Cell Res.* **138**, 109-119. doi:10.1016/0014-4827(82)90096-9

Snell, W. J. and Goodenough, U. W. (2009). Flagellar adhesion, flagellar-generated signaling, and gamete fusion during mating. In *The Chlamydomonas Sourcebook* (ed. G.B. Witman). pp. 369-394. New York: Elsevier.

Snell, W. J. and Moore, W. S. (1980). Aggregation-dependent turnover of flagellar adhesion molecules in *Chlamydomonas* gametes. *J. Cell Biol.* **84**, 203-210. doi:10.1083/jcb.84.1.203

Snell, W. J. and Roseman, S. (1979). Kinetics of adhesion and de-adhesion of *Chlamydomonas* gametes. *J. Biol. Chem.* **254**, 10820-10829. doi:10.1016/S0021-9258(19)86595-X

Truong, M. E., Bilekova, S., Choksi, S. P., Li, W., Bugaj, L. J., Xu, K. and Reiter, J. F. (2021). Vertebrate cells differentially interpret ciliary and extraciliary cAMP. *Cell* **184**, 2911-2926.e18. doi:10.1016/j.cell.2021.04.002

Wachten, D. and Mick, D. U. (2021). Signal transduction in primary cilia - analyzing and manipulating GPCR and second messenger signaling. *Pharmacol. Ther.* **224**, 107836. doi:10.1016/j.pharmthera.2021.107836

Wang, Q. and Snell, W. J. (2003). Flagellar adhesion between mating type *plus* and mating type *minus* gametes activates a flagellar protein-tyrosine kinase during fertilization in *Chlamydomonas*. *J. Biol. Chem.* **278**, 32936-32942. doi:10.1074/jbc.M303261200

Wang, Q., Pan, J. and Snell, W. J. (2006). Intraflagellar transport particles participate directly in cilium-generated signaling in *Chlamydomonas*. *Cell* **125**, 549-562. doi:10.1016/j.cell.2006.02.044

Wen, X., Lai, C. K., Evangelista, M., Hongo, J.-A., de Sauvage, F. J. and Scales, S. J. (2010). Kinetics of hedgehog-dependent full-length Gli3 accumulation in primary cilia and subsequent degradation. *Mol. Cell. Biol.* **30**, 1910-1922. doi:10.1128/MCB.01089-09

Wilson, N. F., Foglesong, M. J. and Snell, W. J. (1997). The *Chlamydomonas* mating type plus fertilization tubule, a prototypic cell fusion organelle: isolation, characterization, and in vitro adhesion to mating type minus gametes. *J. Cell Biol.* **137**, 1537-1553. doi:10.1083/jcb.137.7.1537

Wu, C. T., Hilgendorf, K. I., Bevacqua, R. J., Hang, Y., Demeter, J., Kim, S. K. and Jackson, P. K. (2021). Discovery of ciliary G protein-coupled receptors regulating pancreatic islet insulin and glucagon secretion. *Genes Dev.* **35**, 1243-1255. doi:10.1101/gad.348261.121

Zhang, Y. and Snell, W. J. (1994). Flagellar adhesion-dependent regulation of *Chlamydomonas* adenylyl cyclase in vitro: a possible role for protein kinases in sexual signaling. *J. Cell Biol.* **125**, 617-624. doi:10.1083/jcb.125.3.617

Zhang, Y. H., Ross, E. M. and Snell, W. J. (1991). ATP-dependent regulation of flagellar adenylyl cyclase in gametes of *Chlamydomonas reinhardtii*. *J. Biol. Chem.* **266**, 22954-22959. doi:10.1016/S0021-9258(18)54447-1